

Irvsp: to obtain irreducible representations of electronic states in the VASP

Jiacheng Gao,^{1,2} Quansheng Wu,^{3,4} Clas Persson,⁵ and Zhijun Wang^{1,2,*}

¹*Beijing National Laboratory for Condensed Matter Physics,
and Institute of Physics, Chinese Academy of Sciences, Beijing 100190, China*

²*University of Chinese Academy of Sciences, Beijing 100049, China*

³*Institute of Physics, École Polytechnique Fédérale de Lausanne, CH-1015 Lausanne, Switzerland*

⁴*National Centre for Computational Design and Discovery of Novel Materials MARVEL,
Ecole Polytechnique Fédérale de Lausanne (EPFL), CH-1015 Lausanne, Switzerland*

⁵*Centre for Materials Science and Nanotechnology, Department of Physics,
University of Oslo, P.O. Box 1048 Blindern, NO-0316 Oslo, Norway*

We present an open-source program “*irvsp*”, to compute irreducible representations of electronic states for all 230 space groups with an interface to the Vienna *ab-initio* Simulation Package. This code is fed with plane-wave-based wavefunctions (*e.g.* WAVECAR) and space group operators (listed in OUTCAR), which are generated by the VASP package. This program computes the traces of matrix presentations and determines the corresponding irreducible representations for all energy bands and all the k -points in the three-dimensional Brillouin zone. It also works with spin-orbit coupling (SOC), *i.e.*, for double groups. It is in particular useful to analyze energy bands, their connectivities, and band topology, after the establishment of the theory of topological quantum chemistry. In addition, the code has been also extended to (Wannier-based) tight-binding Hamiltonians. A sister program “*ir2tb*” is presented as well.

I. INTRODUCTION

Topological states [1–9] have been intensively studied in the past decades. During the period, lots of materials have theoretically been proposed to be topological insulators and topological semimetals, based on calculations within the density-functional theory (DFT) [10–16]. Many of them are verified in experiments, and substantially intrigue much interest in theories and experiments, such as three-dimensional (3D) topological insulator Bi_2Se_3 [17–19], Dirac semimetals Na_3Bi [20, 21] and Cd_3As_2 [22, 23], Weyl semimetal TaAs [24–27], topological crystalline insulator SnTe [28, 29] and hourglass material KHgSb [30, 31] *et al.*. To some extent, these topological electron bands are related to a band-inversion feature. Explicitly, there must be a band inversion happened between different irreducible representations (IRs) of the little groups at k -points in the 3D Brillouin zone (BZ) [32]. In the situation of Dirac semimetals or symmetry-protected nodal-line semimetals, it happens on a high-symmetry line or in a high-symmetry plane with different IRs.

Very recently, new insights about band theory have been used to classify all the nontrivial electron band topologies compatible with a given crystal structure [10–12]. In particular, based on the theory of topological quantum chemistry (TQC) [33–36], the topology of a set of isolated electron bands is relied on IRs at the maximal high-symmetry k -points (HSK), as the compatibility relations are solved in Ref. [37], and open accessible on the Bilbao Crystallographic Server (BCS) [38, 39]. The set of maximal HSK points can be found by using the BCS. The determination of the IRs of electron bands at maximal HSK points is of great interest, for which the program – *vasp2trace* – was developed [12]. However, it is not suitable for any non-maximal HSK points.

Generally speaking, in order to obtain the IRs for electron energy bands in crystals, two ingredients are necessary: a) wave-functions (WFs) at k -points and b) character tables (CRTs) for k -little groups. Different versions of the codes can be developed based on the different types of the WFs and conventions of the CRTs. The program *irrep* in the WIEN2k package [40, 41] is a precursor in determining the IRs, which is based on the plane-wave (PW) basis (the part of the WFs outside muffin-tin spheres) and the CRTs of 32 point groups (PNGs). There is an advantage of describing the IRs in terms of the more well-known PNG symmetries, however, the disadvantage is that in many cases k -points on the BZ surface cannot be classified with PNGs for nonsymmorphic crystals. In this paper, the program – *irvsp* – is developed based on the CRTs on the BCS for the VASP package [42]. It originates from the WIEN2k *irrep* code [40, 41] that considers both single- and double groups, analyses of time-reversal symmetry, and

*Electronic address: zjwang11@hotmail.com;

The codes are available in the repository: <https://github.com/zjwang11/irvsp/>.

handles accidental degeneracies. The present code inherits those features but it has been extended to also be able to determine IRs of those special k -points for nonsymmorphic crystals. Hence, the code labels the IRs according to the convention of the BCS notation [39] for all 230 space groups. In fact, it considers both type-I and type-II magnetic space groups. In addition, the code has been also extended to (Wannier-based) tight-binding (TB) Hamiltonians. A sister program – *ir2tb* – is developed also.

This paper is organized as follows. In Section II, we present some basic derivations to compute the traces of matrix presentations in different bases. In Section III, we introduce the general process of the code. In Section IV, we introduce the capabilities of this package. In Section V, we introduce the installation and basic usages. In Section VI, we introduce some examples in order to show how to use *irvsp* to determine the IRs and further explore the topology.

II. METHODS

Space-group symmetry operations, $\mathcal{O}_s = \{R_s|\mathbf{v}_s\}$, consist of two parts: a rotation part R_s and a translation part \mathbf{v}_s . The product of two operations is defined as $\{R_s|\mathbf{v}_s\}\{R_t|\mathbf{v}_t\} = \{R_s R_t|R_s \mathbf{v}_t + \mathbf{v}_s\}$. An operator acting on a function in real space is expressed by $\mathcal{O}f(\mathbf{r}) = f(\mathcal{O}^{-1}\mathbf{r}) = f(R^{-1}\mathbf{r} - R^{-1}\mathbf{v})$ (There is a typo in Section A of the supplementary information of Ref. [12]). The matrix presentations (MPs), O_i^{mn} , can be obtained in the basis of the Bloch wavefunctions $|\psi_{n\mathbf{k}}\rangle$: $O_s^{mn} = \langle\psi_{m\mathbf{k}}|\mathcal{O}_s|\psi_{n\mathbf{k}}\rangle$. The traces of the obtained MPs are the characters, and they are essential to determine the corresponding IRs of the little group (LG) of \mathbf{k} . The LG of \mathbf{k} [$LG(k)$] is defined as a set of space-group operations (SGOs):

$$LG(k) : \{\mathcal{O}_s|R_s\mathbf{k} = \mathbf{k} + \mathbf{G}\}, \text{ with } \mathbf{G} = l\mathbf{g}_1 + m\mathbf{g}_2 + n\mathbf{g}_3, \quad l, m, n \in \mathbb{N} \quad (1)$$

Here, \mathbf{G} could be any integer reciprocal lattice translation ($\mathbf{g}_1, \mathbf{g}_2, \mathbf{g}_3$ are primitive reciprocal lattice vectors). The traces of MPs of SGOs are defined as:

$$\text{Tr}[\mathcal{O}_s] = \sum_n O_s^{nn} \text{ with } O_s^{nn} = \langle\psi_{n\mathbf{k}}|\mathcal{O}_s|\psi_{n\mathbf{k}}\rangle, \quad \mathcal{O}_s \in LG(k). \quad (2)$$

Here, the WFs have to be normalized, $\langle\psi_{n\mathbf{k}}|\psi_{n\mathbf{k}}\rangle = 1$.

Under different bases, the WFs can be expressed in different ways, and the derivations of Eq. (2) are different. Here, we have derived the expressions in two bases: i) PW basis and ii) TB basis. In what follows, symbols in the bold text are vectors, and common bracket notations are employed:

$$\begin{aligned} \langle\mathbf{r}|A\rangle &\equiv A(\mathbf{r}) \\ \langle A|B\rangle &\equiv \int d\mathbf{r} A^*(\mathbf{r})B(\mathbf{r}) \\ \langle\mathbf{r}|\mathbf{k}\rangle &\equiv e^{i\mathbf{k}\cdot\mathbf{r}} \end{aligned}$$

To be convenient, we present the derivations in the cases without the spin degree of freedom. However, the derivations can be easily extended to the cases including SOC, by substituting $R_s \otimes SU_s(2)$ for R_s , where the bases are doubled by the direct product: $\{real\ basis\} \otimes \{|\uparrow\rangle, |\downarrow\rangle\}$. In fact, the code has been designed for both single- and double groups.

A. Plane-wave basis

In a PW basis, wavefunctions/eigenstates are expressed in the basis of plane waves:

$$\psi_{n\mathbf{k}}(\mathbf{r}) = \sum_j C_{\mathbf{k},j} e^{i(\mathbf{k}+\mathbf{G}_j)\cdot\mathbf{r}} \text{ with } \langle\mathbf{k} + \mathbf{G}_i|\mathbf{k} + \mathbf{G}_j\rangle = \delta_{ij} \quad (3)$$

The coefficients ($C_{\mathbf{k},j}$) are usually computed in the *ab-initio* calculations and output by the DFT package (*e.g.* VASP). The SGOs acting on WFs are derived as:

$$\begin{aligned}
\mathcal{O}_s \psi_{n\mathbf{k}}(\mathbf{r}) &= \sum_j C_{\mathbf{k},j} e^{i(\mathbf{k}+\mathbf{G}_j)\cdot(R_s^{-1}\mathbf{r}-R_s^{-1}\mathbf{v}_s)} \\
&= \sum_j C_{\mathbf{k},j} e^{iR_s(\mathbf{k}+\mathbf{G}_j)\cdot(\mathbf{r}-\mathbf{v}_s)} \\
&= \sum_j C_{\mathbf{k},j} e^{i(\mathbf{k}+\mathbf{G}_{j'})\cdot(\mathbf{r}-\mathbf{v}_s)} \text{ with } \mathbf{k} + \mathbf{G}_{j'} \equiv R_s(\mathbf{k} + \mathbf{G}_j) \\
&= e^{-i\mathbf{k}\cdot\mathbf{v}_s} \sum_j C_{\mathbf{k},j} e^{-i\mathbf{G}_{j'}\cdot\mathbf{v}_s} e^{i(\mathbf{k}+\mathbf{G}_{j'})\cdot\mathbf{r}} \text{ with } \mathbf{G}_{j'} \equiv R_s(\mathbf{k} + \mathbf{G}_j) - \mathbf{k}
\end{aligned}$$

Then, Eq. (2) can be written as:

$$\langle \psi_{n\mathbf{k}} | \mathcal{O}_s | \psi_{n\mathbf{k}} \rangle = e^{-i\mathbf{k}\cdot\mathbf{v}_s} \sum_j C_{\mathbf{k},j}^* C_{\mathbf{k},j} e^{-i\mathbf{G}_{j'}\cdot\mathbf{v}_s} \text{ with } \mathbf{G}_{j'} \equiv R_s(\mathbf{k} + \mathbf{G}_j) - \mathbf{k} \quad (4)$$

The program “irvsp” is developed based on the above derivations with the interface to VASP. However, it should work for any PW-based code, once a proper interface is made.

B. Tight-binding basis

In a TB Hamiltonian, WFs are expressed in the basis of localized (Wannier) orbitals: $|\mathbf{0}, \mu\alpha\rangle \equiv \phi_\alpha^\mu(\mathbf{r}) \equiv \phi_\alpha(\mathbf{r} - \tau_\mu)$ and $|\mathbf{L}_j, \mu\alpha\rangle \equiv \phi_\alpha(\mathbf{r} - \mathbf{L}_j - \tau_\mu)$, where μ label the atoms, α label the orbitals, \mathbf{L}_j label the lattice vectors in 3D crystals, and τ_μ label the positions of atoms in a home unit cell. At a given k -point, WFs are given as:

$$\psi_{n\mathbf{k}}(\mathbf{r}) = \sum_{\mu\alpha} C_{\mu\alpha,\mathbf{k}}^n \phi_{\alpha\mathbf{k}}^\mu(\mathbf{r}) \text{ where } n \text{ is a band index,} \quad (5)$$

$$\phi_{\alpha\mathbf{k}}^\mu(\mathbf{r}) = \sum_j \phi_\alpha(\mathbf{r} - \tau_\mu - \mathbf{L}_j) e^{i\mathbf{k}\cdot(\mathbf{L}_j + \tau_\mu)}, \langle \phi_{\beta\mathbf{k}}^{\mu'} | \phi_{\alpha\mathbf{k}}^\mu \rangle = \delta_{\mu\mu'} \delta_{\alpha\beta} \quad (6)$$

The states $\phi_{\alpha\mathbf{k}}^\mu(\mathbf{r})$ are the Fourier transformations of the local orbitals $\phi_\alpha^\mu(\mathbf{r})$, as shown in Eq. (6). The coefficients are obtained as the eigenvectors of the TB Hamiltonian: $H_{\mu'\beta,\mu\alpha}(\mathbf{k}) = \sum_j e^{i\mathbf{k}\cdot(\mathbf{L}_j + \tau_\mu - \tau_{\mu'})} \langle \mathbf{0}, \mu'\beta | \hat{H} | \mathbf{L}_j, \mu\alpha \rangle$. The rotational symmetries R_s acting on the local orbitals $[\phi_\alpha(\mathbf{r})]$ of the μ site are given as:

$$\widehat{R}_s \phi_\alpha(\mathbf{r}) \equiv R_s \phi_\alpha(\mathbf{r}) = \sum_\beta \phi_\beta(\mathbf{r}) D_{\beta\alpha}^{s,\mu} \quad (7)$$

These D -matrices are explicitly given in Table S3 in the Appendix. Under the basis of real spherical harmonic functions with different total angular momenta (integer l), these D -matrices are real.

The SGOs acting on the states $\phi_{\alpha\mathbf{k}}^{\mu}(\mathbf{r})$ are given below:

$$\begin{aligned}
\mathcal{O}_s \phi_{\alpha\mathbf{k}}^{\mu}(\mathbf{r}) &= \phi_{\alpha\mathbf{k}}^{\mu}(R_s^{-1}\mathbf{r} - R_s^{-1}\mathbf{v}_s) \\
&= \sum_j \phi_{\alpha}(R_s^{-1}\mathbf{r} - R_s^{-1}\mathbf{v}_s - \tau_{\mu} - \mathbf{L}_j) e^{i\mathbf{k}\cdot(\mathbf{L}_j + \tau_{\mu})} \\
&= \sum_j \phi_{\alpha}(R_s^{-1}[\mathbf{r} - \mathbf{v}_s - R_s\tau_{\mu} - R_s\mathbf{L}_j]) e^{i\mathbf{k}\cdot(\mathbf{L}_j + \tau_{\mu})} \\
&= \sum_j \widehat{R}_s \phi_{\alpha}[\mathbf{r} - \mathbf{v}_s - R_s\tau_{\mu} - R_s\mathbf{L}_j] e^{i(R_s\mathbf{k})\cdot R(\mathbf{L}_j + \tau_{\mu})} \text{ with } \widehat{R}_s \phi_{\alpha}(\mathbf{r}) \equiv \sum_{\beta} \phi_{\beta}(\mathbf{r}) D_{\beta\alpha}^{s,\mu} \\
&= e^{-i(R_s\mathbf{k}\cdot\mathbf{v}_s)} \sum_j \widehat{R}_s \phi_{\alpha}[\mathbf{r} - (\mathbf{v}_s + R_s\tau_{\mu}) - R_s\mathbf{L}_j] e^{i(R_s\mathbf{k})\cdot[R_s\mathbf{L}_j + (R_s\tau_{\mu} + \mathbf{v}_s)]} \\
&= e^{-i(R_s\mathbf{k}\cdot\mathbf{v}_s)} \sum_j \widehat{R}_s \phi_{\alpha}[\mathbf{r} - (\tau_{\mu'} + \mathbf{L}_0^i) - R_s\mathbf{L}_j] e^{i(R_s\mathbf{k})\cdot[R_s\mathbf{L}_j + (\tau_{\mu'} + \mathbf{L}_0^i)]} \text{ using } \mathbf{v}_s + R_s\tau_{\mu} = \mathbf{L}_0^i + \tau_{\mu'} \\
&= e^{-i(R_s\mathbf{k}\cdot\mathbf{v}_s)} \sum_{j'} \widehat{R}_s \phi_{\alpha}[\mathbf{r} - \tau_{\mu'} - \mathbf{L}_{j'}] e^{i(R_s\mathbf{k})\cdot[\mathbf{L}_{j'} + \tau_{\mu'}]} \text{ with } \mathbf{L}_{j'} = \mathbf{L}_0^i + R_s\mathbf{L}_j \\
&= e^{-i(R_s\mathbf{k}\cdot\mathbf{v}_s)} \sum_{\beta} \phi_{\beta,R_s\mathbf{k}}^{\mu'}(r) D_{\beta\alpha}^{s,\mu}
\end{aligned}$$

Thus, Eq. (2) is written as:

$$\langle \psi_{n\mathbf{k}} | \mathcal{O}_s | \psi_{n\mathbf{k}} \rangle = e^{-i(R_s\mathbf{k}\cdot\mathbf{v}_s)} \sum_{\alpha\mu,\beta} C_{\mu'\beta}^{m*} e^{i(R_s\mathbf{k}-\mathbf{k})\cdot\tau_{\mu'}} D_{\beta\alpha}^{s,\mu} C_{\mu\alpha}^n \text{ with } \mathbf{v}_s + R_s\tau_{\mu} = \mathbf{L}_0^i + \tau_{\mu'} \quad (8)$$

In a matrix format,

$$\langle \psi_{n\mathbf{k}} | \mathcal{O}_s | \psi_{n\mathbf{k}} \rangle = e^{-i(R_s\mathbf{k}\cdot\mathbf{v}_s)} \left[\overline{C^\dagger V(R_s\mathbf{k} - \mathbf{k}) DC} \right]_{nn} \quad (9)$$

$$\text{with } \overline{V}(\mathbf{k})_{\mu'\beta,\mu\alpha} = e^{i\mathbf{k}\cdot\tau_{\mu'}} \delta_{\mu\mu'} \delta_{\alpha\beta}, \quad \overline{C}_{\mu\alpha,n} = C_{\mu\alpha}^n, \quad \overline{D}_{\mu'\beta,\mu\alpha} = \begin{cases} D_{\beta\alpha}^{s,\mu} & \text{when } \mathbf{v}_s + R_s\tau_{\mu} = \mathbf{L}_0^i + \tau_{\mu'}; \\ 0 & \text{otherwise.} \end{cases} \quad (10)$$

Based on the above derivations, the code has been extended to the TB basis. The sister program is called “ir2tb”. Users must provide two files: *case_hr.dat* and *tbbox.in*. The file called *case_hr.dat*, containing the TB parameters, may be generated by the software Wannier90 [43, 44] with symmetrization [45–47], or generated by users with a toy TB model, or generated from Slater-Koster method [48] or discretization of $k \cdot p$ model onto a lattice [49]. The other file *tbbox.in* is the master input file for “ir2tb”. It should be given consistently with the TB parameters in *case_hr.dat*. An example of *tbbox.in* is given for Bi₂Se₃ in the Appendix.

III. GENERAL PROCESS OF THE CODE

In the main text, we are mainly focused on “irvsp”, which is based on the PW basis with an interface to the VASP package [42]. One can check more details for “ir2tb” in the Appendix.

A. Wavefunctions at k -points

In the VASP package, the all-electron wave-function is obtained by acting a linear operator \mathcal{T} on the pseudo wave-function: $|\psi_{n\mathbf{k}}\rangle = \mathcal{T} |\tilde{\psi}_{n\mathbf{k}}\rangle$. The linear operator can be written explicitly as: $\mathcal{T} = \mathbf{1} + \sum_i \left(|\phi_i\rangle - |\tilde{\phi}_i\rangle \right) \langle p_i|$, where $|\phi_i\rangle$ ($|\tilde{\phi}_i\rangle$) is a set of all-electron (pseudo) partial waves around each atom and $|p_i\rangle$ is a set of corresponding projector functions on each atom within an augmentation region ($r < R_0$), where R_0 is the core part for each atom. The pseudo-wavefunction is expanded in the plane waves:

$$\tilde{\psi}_{n\mathbf{k}}(\vec{r}) \equiv \langle r | \tilde{\psi}_{n\mathbf{k}} \rangle = \sum_{\vec{G}} C_{n,\mathbf{k}+\vec{G}} e^{i(\mathbf{k}+\vec{G})\cdot\vec{r}} \quad (11)$$

where \vec{G} vectors are determined by the condition $\frac{\hbar^2}{2m_e}(\mathbf{k} + \vec{G})^2 < E_{cutoff}$ with a cutoff E_{cutoff} . It is worthy noting that $|\tilde{\psi}_{n\mathbf{k}}\rangle$ are sufficient for the calculations of the traces of MPs of SGOs.

Since the pseudo-wavefunctions $|\tilde{\psi}_{n\mathbf{k}}\rangle$ are usually not normalized, they have to be renormalized before their traces can be computed via Eq. (2). The coefficients ($C_{\mathbf{k}+\vec{G}_j}$) are output in WAVECAR by VASP. In the program, they are read by the subroutine: *wave_data.f90*. In the SOC case, the $C_{\mathbf{k}+\vec{G}_j,\uparrow}$ and $C_{\mathbf{k}+\vec{G}_j,\downarrow}$ are stored in the complex variables *coeffa*(:) and *coeffb*(:). In the case without SOC, the $C_{\mathbf{k}+\vec{G}_j}$ are stored in *coeffa*(:), while *coeffb*(:) are invalid (set to be zero).

TABLE I: A brief summary of key subroutines

File	Description	Input
wave_data.f90	reading the coefficients.	WAVECAR
init.f90	reading lattice vectors and space group operators, and setting up the Z and Z^{-1} matrices.	OUTCAR
kgroup.f90	determining the \mathbf{k} -little groups.	
nonsymm.f90	retrieving the character tables from the BCS	
chrct.f90	computing the traces through the Eq. (4), and determining the IRs	

B. Symmetry operators of a crystal

Instead of generating space group operators from a crystal structure (*i.e.*, POSCAR), the program reads the SGOs directly from the standard output of VASP (*i.e.*, OUTCAR), which is done by the subroutine: *init.f90*. In other words, the SGOs are generated by the VASP package (*e.g.* with ISYM = 1 or 2 in INCAR for vasp.5.3.3), which are listed below the line of ‘Space group operators’ in OUTCAR. Fig. 1 shows an example of Bi_2Se_3 for the SGOs of space group (SG) 166. They are given by $Det (\pm 1)$, ω , and $\vec{n} (n_x, n_y, n_z)$ and $\mathbf{v} (v_1\mathbf{t}_1, v_2\mathbf{t}_2, v_3\mathbf{t}_3)$ with $\mathbf{t}_1, \mathbf{t}_2, \mathbf{t}_3$ primitive lattice vectors. The -1 value of Det indicates that the operator is a roto-inversion. Actually, the listed SGOs depend on the lattice vectors. Primitive lattice vectors ($\mathbf{t}_1, \mathbf{t}_2, \mathbf{t}_3$) and primitive reciprocal lattice vectors ($\mathbf{g}_1, \mathbf{g}_2, \mathbf{g}_3$) are read from OUTCAR, also shown in Fig. 2 for Bi_2Se_3 . The O(3) and SU(2) matrix presentations are generated in the spin-1 (under the basis of $\{\mathbf{x}, \mathbf{y}, \mathbf{z}\}$) and spin-1/2 (under the basis of $\{\uparrow, \downarrow\}$) spaces, respectively:

$$R(\omega, \vec{n}) = Det \cdot e^{-i\omega(\vec{n} \cdot \vec{L})}, L_x = \begin{pmatrix} 0 & 0 & 0 \\ 0 & 0 & -i \\ 0 & i & 0 \end{pmatrix}, L_y = \begin{pmatrix} 0 & 0 & i \\ 0 & 0 & 0 \\ -i & 0 & 0 \end{pmatrix}, L_z = \begin{pmatrix} 0 & -i & 0 \\ i & 0 & 0 \\ 0 & 0 & 0 \end{pmatrix}; \quad (12)$$

$$S(\omega, \vec{n}) = e^{-i\omega(\vec{n} \cdot \vec{S})}, S_x = \frac{\sigma_x}{2} = \frac{1}{2} \begin{pmatrix} 0 & 1 \\ 1 & 0 \end{pmatrix}, S_y = \frac{\sigma_y}{2} = \frac{1}{2} \begin{pmatrix} 0 & -i \\ i & 0 \end{pmatrix}, S_z = \frac{\sigma_z}{2} = \frac{1}{2} \begin{pmatrix} 1 & 0 \\ 0 & -1 \end{pmatrix}. \quad (13)$$

Space group operators:									
irotd	det(A)	alpha	n_x	n_y	n_z	tau_x	tau_y	tau_z	
1	1.000000	0.000000	1.000000	0.000000	0.000000	0.000000	0.000000	0.000000	0.000000
2	-1.000000	0.000000	1.000000	0.000000	0.000000	0.000000	0.000000	0.000000	0.000000
3	1.000000	180.000000	0.866025	0.500000	0.000000	0.000000	0.000000	0.000000	0.000000
4	-1.000000	180.000000	0.866025	0.500000	0.000000	0.000000	0.000000	0.000000	0.000000
5	1.000000	120.000000	0.000000	0.000000	-1.000000	0.000000	0.000000	0.000000	0.000000
6	-1.000000	120.000000	0.000000	0.000000	-1.000000	0.000000	0.000000	0.000000	0.000000
7	1.000000	179.999999	0.000000	1.000000	0.000000	0.000000	0.000000	0.000000	0.000000
8	-1.000000	179.999999	0.000000	1.000000	0.000000	0.000000	0.000000	0.000000	0.000000
9	1.000000	120.000000	0.000000	0.000000	1.000000	0.000000	0.000000	0.000000	0.000000
10	-1.000000	120.000000	0.000000	0.000000	1.000000	0.000000	0.000000	0.000000	0.000000
11	1.000000	180.000000	0.866025	-0.500000	0.000000	0.000000	0.000000	0.000000	0.000000
12	-1.000000	180.000000	0.866025	-0.500000	0.000000	0.000000	0.000000	0.000000	0.000000

FIG. 1: Screenshot of OUTCAR, showing the space group operators of Bi_2Se_3 generated by VASP.

direct lattice vectors			reciprocal lattice vectors		
1.194537707	-2.069000000	9.546666657	0.139523990	-0.241662639	0.034916201
1.194537707	2.069000000	9.546666657	0.139523990	0.241662639	0.034916201
-2.389075414	0.000000000	9.546666657	-0.279047979	0.000000000	0.034916201

FIG. 2: Screenshot of OUTCAR, showing the lattice vectors and reciprocal lattice vectors of Bi_2Se_3 which are used in VASP.

In 3D crystals, it is more convenient to use matrix presentations in the lattices of $(\mathbf{t}_1, \mathbf{t}_2, \mathbf{t}_3)$ in real space and in reciprocal lattices of $(\mathbf{g}_1, \mathbf{g}_2, \mathbf{g}_3)$ in momentum space. They are given in the following convention:

$$\vec{v} = \mathbf{t}_1 v_1 + \mathbf{t}_2 v_2 + \mathbf{t}_3 v_3 = (\mathbf{t}_1, \mathbf{t}_2, \mathbf{t}_3) \begin{pmatrix} v_1 \\ v_2 \\ v_3 \end{pmatrix}, \quad (\mathbf{t}_1, \mathbf{t}_2, \mathbf{t}_3) \equiv \begin{pmatrix} t_{1x} & t_{2x} & t_{3x} \\ t_{1y} & t_{2y} & t_{3y} \\ t_{1z} & t_{2z} & t_{3z} \end{pmatrix}; \quad (14)$$

$$\vec{k} = k_1 \mathbf{g}_1 + k_2 \mathbf{g}_2 + k_3 \mathbf{g}_3 = (k_1, k_2, k_3) \begin{pmatrix} \mathbf{g}_1 \\ \mathbf{g}_2 \\ \mathbf{g}_3 \end{pmatrix}, \quad \begin{pmatrix} \mathbf{g}_1 \\ \mathbf{g}_2 \\ \mathbf{g}_3 \end{pmatrix} \equiv \begin{pmatrix} g_{1x} & g_{1y} & g_{1z} \\ g_{2x} & g_{2y} & g_{2z} \\ g_{3x} & g_{3y} & g_{3z} \end{pmatrix}. \quad (15)$$

$$\text{with } \begin{pmatrix} \mathbf{g}_1 \\ \mathbf{g}_2 \\ \mathbf{g}_3 \end{pmatrix} (\mathbf{t}_1, \mathbf{t}_2, \mathbf{t}_3) = 2\pi \mathbb{I}_{3 \times 3}$$

The rotational symmetry operators acting on the vectors are transformed as:

$$R\vec{v} = (\mathbf{t}_1, \mathbf{t}_2, \mathbf{t}_3) Z \begin{pmatrix} v_1 \\ v_2 \\ v_3 \end{pmatrix}, \quad R\vec{k} = (k_1, k_2, k_3) Z^{-1} \begin{pmatrix} \mathbf{g}_1 \\ \mathbf{g}_2 \\ \mathbf{g}_3 \end{pmatrix}; \quad (16)$$

$$R(\mathbf{t}_1, \mathbf{t}_2, \mathbf{t}_3) = (\mathbf{t}_1, \mathbf{t}_2, \mathbf{t}_3) Z, \quad (17)$$

Thus, rotational matrix presentations in the lattice vectors are 3×3 integer matrices (Z), which are defined in Eq. (17). Instead of the real R -matrices in Cartesian coordinates in Eq. (12), the integer matrices, Z and Z^{-1} , are actually stored and used throughout the code, which are all set in the subroutine: *init.f90*

If one wants to do some sub-space-group symmetry calculations, one can modify the SGOs in OUTCAR and give the correct space group number accordingly. For example, if one only wants to know parity eigenvalues of the energy bands, one can change the list of SGOs with only two lines (*i.e.*, identity and inversion symmetry) and give space group 2 to run *irvsp*.

C. Little group of a certain k -point

The eigen-wavefunctions at a certain k -point only support the IRs of the little group of \mathbf{k} , $LG(k)$. Therefore, for any given k -point, the program has to determine the \mathbf{k} -little group $LG(k)$ first. This is done in the subroutine: *kgroup.f90*. The $LG(k)$ are defined by Eq. (1). In the program, the integer matrices Z^{-1} and Eq. (16) in momentum space are used.

D. Character tables for k -little groups

Currently, there are two conventions of CRTs for k -little groups. In the first convention, the k points are labeled by the IRs of the PNGs, since IRs of the space group can be expressed as IRs of the corresponding point group multiplied by a phase factor. They are suitable either for symmorphic space groups, or the inner k -points (not on the BZ boundary/surface) for the non-symmorphic space groups. The CRTs of PNGs are given in the Ref. [50, 51], which have been implemented in the program *irrep* of the WIEN2k package [40, 41]. In the second convention, all the CRTs for k -points of all 230 space groups are listed on the BCS [39]. To compare the computed traces with these characters, one do not need to distinguish symmorphic and nonsymmorphic space groups at all. Therefore, the program “*irvsp*” is valid for all 230 space groups. The CRTs are retrieved from the inputs of the BCS, which are done by the subroutine: *nonsymm.f90*.

As an example, consider the Γ point of Bi_2Se_3 . Fig. 3 shows the CRT of the point group D_{3d} in the PNG convention. Fig. 4 shows the CRT in the BCS convention. Both tables can be used to determine the IRs at Γ in SG 166. In the

table of Fig. 4, the first and two columns show the reality and the BCS labels of IRs, respectively. The following columns indicate the characters of different SGOs. The reality of an IR is given by the definition [50, 51]:

$$\frac{1}{|G|} \sum_{j=1}^{|G|} \chi(G_j^2) = \begin{cases} 1 & \text{potentially real, case (a)} \\ 0 & \text{essentially complex, case (b)} \\ -1 & \text{pseudo-real, case (c)} \end{cases} \quad (18)$$

where G_j is an element of a group G , and $|G|$ is the rank of the group G . In case (a), the IR is equivalent to its complex representation, and also equivalent to a real representation. In case (b), the IR is not equivalent to its complex representation. In case (c), the IR is equivalent to its complex representation, but not to a real representation.

In the type-II magnetic space groups (MSGs), including pure time-reversal symmetry (TRS), the existence of antiunitary SGOs in the k -little group is indicated at the beginning of the character table (Fig. 4). In the absence of SOC (integer spin), TRS doubles the degeneracy of IRs in cases (b) and (c); while in the presence of SOC (half-integer spin), it doubles the degeneracy of the IRs in cases (a) and (b).

```

The point group is D3d
12 symmetry operations in 6 classes
Table 55 on page 58 in Koster et al [7]
Table 42.4 on page 371 in Altmann et al [8]

```

		E	2C3	3C2	I	2IC3	3IC2
G1+	A1g	1	1	1	1	1	1
G2+	A2g	1	1	-1	1	1	-1
G3+	Eg	2	-1	0	2	-1	0
G1-	A1u	1	1	1	-1	-1	-1
G2-	A2u	1	1	-1	-1	-1	1
G3-	Eu	2	-1	0	-2	1	0

G4+	E1/2g	2	1	0	2	1	0
G5+	1E3/2g	1	-1	i	1	-1	i
G6+	2E3/2g	1	-1	-i	1	-1	-i
G4-	E1/2u	2	1	0	-2	-1	0
G5-	1E3/2u	1	-1	i	-1	1	-i
G6-	2E3/2u	1	-1	-i	-1	1	i

FIG. 3: The character table of point group D_{3d} , which is used to determine the IRs (*i.e.*, PNG convention) for the energy bands at Γ of Bi_2Se_3 in *irrep* of the WIEN2k package.

```

The k-point name is GM
12 symmetry operations (module lattice translations) in the GM-little group of space group 166
We do NOT classify the elements into classes.
Tables can be found on website: http://www.cryst.ehu.es/.

```

1	GM : kname	0.00	0.00	0.00	0.00	0.00	0.00	0.00	0.00	0.00	0.00	0.00	0.00
1	GM1-	1.00+0.00i	1.00+0.00i	1.00+0.00i	1.00+0.00i	1.00+0.00i	1.00+0.00i	1.00+0.00i	1.00+0.00i	1.00+0.00i	1.00+0.00i	1.00+0.00i	1.00+0.00i
1	GM2+	1.00+0.00i	1.00+0.00i	1.00+0.00i	1.00+0.00i	1.00+0.00i	1.00+0.00i	1.00+0.00i	1.00+0.00i	1.00+0.00i	1.00+0.00i	1.00+0.00i	1.00+0.00i
1	GM2-	1.00+0.00i	1.00+0.00i	1.00+0.00i	-1.00+0.00i	-1.00+0.00i	-1.00+0.00i	-1.00+0.00i	-1.00+0.00i	-1.00+0.00i	-1.00+0.00i	-1.00+0.00i	-1.00+0.00i
1	GM3+	2.00+0.00i	-1.00+0.00i	-1.00+0.00i	0.00+0.00i	0.00+0.00i	0.00+0.00i	2.00+0.00i	-1.00+0.00i	-1.00+0.00i	0.00+0.00i	0.00+0.00i	0.00+0.00i
1	GM3-	2.00+0.00i	-1.00+0.00i	-1.00+0.00i	0.00+0.00i	0.00+0.00i	0.00+0.00i	-2.00+0.00i	1.00+0.00i	1.00+0.00i	0.00+0.00i	0.00+0.00i	0.00+0.00i

0	GM4	1.00+0.00i	-1.00+0.00i	-1.00+0.00i	0.00-1.00i	0.00+1.00i	0.00-1.00i	1.00+0.00i	-1.00+0.00i	-1.00+0.00i	0.00-1.00i	0.00+1.00i	0.00-1.00i
0	GM5	1.00+0.00i	-1.00+0.00i	-1.00+0.00i	0.00+1.00i	0.00-1.00i	0.00+1.00i	1.00+0.00i	-1.00+0.00i	-1.00+0.00i	0.00+1.00i	0.00-1.00i	0.00+1.00i
0	GM6	1.00+0.00i	-1.00+0.00i	-1.00+0.00i	0.00-1.00i	0.00+1.00i	0.00-1.00i	-1.00+0.00i	1.00+0.00i	1.00+0.00i	0.00+1.00i	0.00-1.00i	0.00+1.00i
0	GM7	1.00+0.00i	-1.00+0.00i	-1.00+0.00i	0.00+1.00i	0.00-1.00i	0.00+1.00i	-1.00+0.00i	1.00+0.00i	1.00+0.00i	0.00-1.00i	0.00+1.00i	0.00-1.00i
-1	GM8	2.00+0.00i	1.00+0.00i	1.00+0.00i	0.00+0.00i	0.00+0.00i	0.00+0.00i	2.00+0.00i	1.00+0.00i	1.00+0.00i	0.00+0.00i	0.00+0.00i	0.00+0.00i
-1	GM9	2.00+0.00i	1.00+0.00i	1.00+0.00i	0.00+0.00i	0.00+0.00i	0.00+0.00i	-2.00+0.00i	-1.00+0.00i	-1.00+0.00i	0.00+0.00i	0.00+0.00i	0.00+0.00i

FIG. 4: The character table of Γ -little group in SG 166 on the BCS, which is used to determine the IRs (*i.e.*, BCS convention) for the energy bands at Γ of Bi_2Se_3 in the program *irvsp*.

E. Determination of irreducible representations

After the normalization of the plane-wave-based pseudo-wavefunctions in VASP, the traces of matrix presentations of SGOs can be computed via Eq. (4), which are done in the subroutine 'chrct.f90'. By comparing the obtained traces and the characters of the CRTs, the IRs are determined and labeled in the convention of the BCS notations.

TABLE II: Four versions of “irvsp” are implemented. The first column indicates the version number, the second column shows the convention of reference CRTs, and the brief description is followed in the last column.

Version	CRTs	Brief description
version I	PNG	It resembles an analogue of the program <i>irrep</i> in the WIEN2k package.
version II	BCS	It works for the k -points, where version I does not work.
version III	PNG&BCS	It combines version I and version II.
version IV (default)	BCS	It works for all the k -points and all 230 space groups, including <i>nonsymmorphic</i> space groups. All the IRs are labeled in the convention of the BCS notation.

IV. CAPABILITIES OF “IRVSP”

In the study of the property of a material, the determination of IRs of computed electron bands is of great interest to diagnose the band crossing/anti-crossing, degeneracy and band topology. The program is aimed to get the IRs for all the bands at all the k -points for all 230 space group. In particular, it also works for the k -points on the boundary of the 3D BZ in nonsymmorphic space groups. Four versions of “irvsp” are implemented, as shown in Table II. Version I works similarly (using some subroutines directly) as “irrep” in the WIEN2k package (using some subroutines directly) and presents the IRs with PNG symmetries. This version can thus not classify the special k -points on the boundary of the Brillouin zone of nonsymmorphic crystals, that is, when $\exp[-ik(R_s v_t + v_s)] \neq 1$ for some O_s and O_t in $\text{LG}(k)$. Version II has been extended to classify the IRs at also all BZ surface k -points for nonsymmorphic space groups. Version III combines version I and II. In the (default) version IV, it works for all the k -points and all 230 space groups (*i.e.*, both type-I and type-II MSGs). Without additional information, the program “irvsp” refers to version IV throughout the work. All the IRs are labeled in the convention of the BCS notation. The obtained IRs at the maximal HSK points can be directly compared with the elementary band representations (EBRs) of the TQC theory, to further check the topology of a set of bands in materials.

V. INSTALLATION AND USAGE

In this section, we will show how to install and use the “irvsp” software package. This program is an open source free software package. It is released on Github under the Standard CPC licence, <http://cpc.cs.qub.ac.uk/licence/licence.html>, and it can be downloaded directly from the public code repository: https://github.com/zjwang11/irvsp/blob/master/src_irvsp_v2.tar.gz.

To build and install “irvsp”, only a Fortran 90 compiler is needed. The downloaded “irvsp” software package is likely a compressed file with a zip or tar.gz suffix. One should uncompress it first, then move into the `src_irvsp_v2` folder. After setting up the Fortran compiler in the ‘Makefile’ file, the executable binary *irvsp* will be compiled by typing the following command in the current directory (`src_irvsp_v2`):

```
$ make
```

Before running *irvsp*, the user must provide two consistent files: WAVECAR and OUTCAR. The two files are generated by the VASP package in fixed format. It is designed to be simple and user friendly. After a running of VASP with WAVECAR and OUTCAR output, the program *irvsp* can be run immediately in the same folder. Giving a correct space group number ($sgn \in [1, 230]$) [and a version number ($nv \in \{1, 2, 3, 4\}$)], the program can be executed by the following command:

```
$ irvsp -sgn sgn [ -v nv ] > outir &
```

VI. EXAMPLES

In the WIEN2k package, the program *irrep* classifies the IRs in PNG symmetries, which then excludes the possibility to describe certain BZ surface k -points for nonsymmorphic crystals. Very recently, the codes *vasp2trace* and *CheckTopologicalMat*, designed for TQC in the Ref. [12], have been used (tested) in all 230 space groups and uncover thousands of new materials with topological electron bands. However, they are not suitable for non-maximal HSK points. Therefore, the demand to determine the IRs for all the k -point and all 230 space groups is still unsatisfied. With the CRTs from the BCS, the program – *irvsp* – is developed to meet this demand. In this work, we take

topological materials PdSb₂ and Bismuth as examples to show how to study topological properties of new materials with “irvsp”.

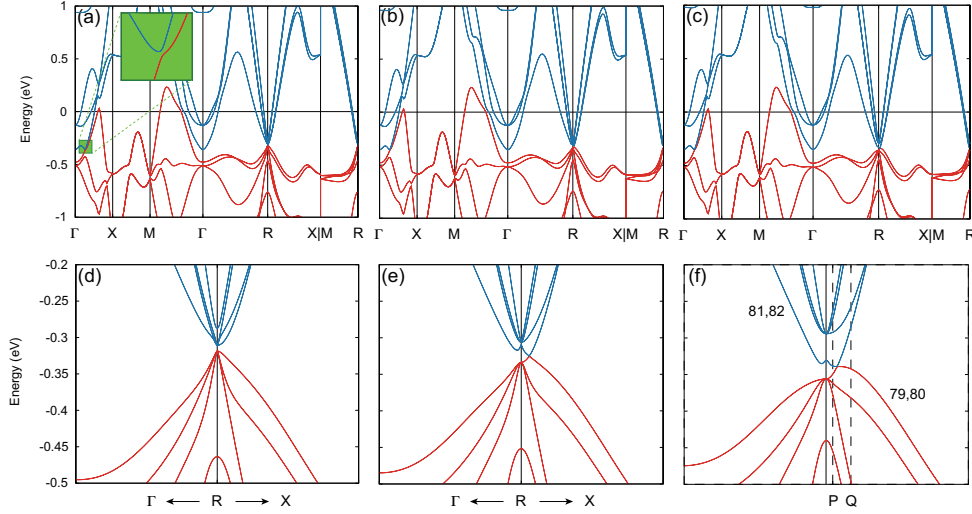


FIG. 5: Electronic band structures of PdSb₂ without strain, with 0.3% (b) and 0.62% tensile strains. Panels (d), (e), and (f) are the zoom-in plots of (a) (b) (c) near the R point. In our calculations, the total number of electrons is 80. Therefore, the first 80 bands are regarded as valence bands (red-colored), while the other energetically higher bands are considered as conduction bands (blue-colored).

A. PdSb₂

PdSb₂ was predicted to be a candidate hosting sixfold-degenerate fermions because of the nonsymmorphic symmetry [52, 53]. The crystal of PdSb₂ is a cubic structure of SG 205. We adopt the experimental lattice constant a [54–56] and fully relax the coordinate of inner atom positions. In the obtained band structure (BS) of Fig. 5(a) along the high-symmetry lines, we note that there is a tiny gap (~ 10 meV) between two sixfold degeneracies at R . Then, we want to know the corresponding IRs of two sixfold degeneracies and how they are going to evolve under strains. For this purpose, we performed the calculations with different tensile strains (*i.e.*, $\Delta a/a = 0.3\%$ and $\Delta a/a = 0.62\%$). Their electronic band structures are shown in Figs. 5 (b) and (c), respectively. Comparing with the strain-free BS in Fig. 5(a), we find that the overall BS doesn’t change much, except for the R point. The zoom-in plots around

(a)							(b)								
bnd	ndg	eigval	E	...	15	...	24	bnd	ndg	eigval	E	...	15	...	24
...								...							
73	2	8.418482	2.00+0.00i	...	-2.00+0.00i	...	-1.00+0.00i =R8 + R9	73	2	8.297689	2.00+0.00i	...	-2.00+0.00i	...	-1.00+0.00i =R8 + R9
75	6	8.563493	6.00+0.00i	...	2.00+0.00i	...	0.00+0.00i =R11 + R11	75	6	8.415820	6.00+0.00i	...	-2.00+0.00i	...	0.00+0.00i =R10 + R10
81	6	8.571287	6.00+0.00i	...	-2.00+0.00i	...	-0.00+0.00i =R10 + R10	81	2	8.440170	2.00+0.00i	...	2.00+0.00i	...	1.00+0.00i =R5 + R6
87	2	8.594609	2.00+0.00i	...	2.00+0.00i	...	1.00+0.00i =R5 + R6	83	6	8.443062	6.00+0.00i	...	2.00+0.00i	...	0.00+0.00i =R11 + R11

(c)							
bnd	ndg	eigval	E	...	15	...	24
...							
73	2	8.178326	2.00+0.00i	...	-2.00+0.00i	...	-1.00+0.00i =R8 + R9
75	6	8.262436	6.00+0.00i	...	-2.00+0.00i	...	0.00+0.00i =R10 + R10
81	2	8.287815	2.00+0.00i	...	2.00+0.00i	...	1.00+0.00i =R5 + R6
83	6	8.324102	6.00+0.00i	...	2.00+0.00i	...	0.00+0.00i =R11 + R11

FIG. 6: The IRs at R are determined by the program “irvsp”. The CRT of the R -little group is shown in Fig. S1 in the appendix. The first three columns stands for the band indices, degeneracies, and the energies (without subtracting the Fermi energy E_F). The following columns indicates the traces (characters) of the corresponding space group operators (listed as “E, 2, ..., 24”). The assigned IR labels are output to the right of the equality sign “=”. The (a), (b), (c) panels are the results of the three crystal structures, respectively.

(a)										(b)									
bnd	ndg	eigval	E	15						bnd	ndg	eigval	E	15					
1	4	-1.597312	4.00+0.00i	-0.00+0.00i	=S3	+ S3	+ S4	+ S4	1	4	-1.615810	4.00+0.00i	-0.00+0.00i	=S3	+ S3	+ S4	+ S4		
5	4	-1.594935	4.00+0.00i	-0.00+0.00i	=S3	+ S3	+ S4	+ S4	5	4	-1.592474	4.00+0.00i	-0.00+0.00i	=S3	+ S3	+ S4	+ S4		
...																			
77	2	8.255055	2.00+0.00i	-2.00+0.00i	=S3	+ S3			77	2	8.236502	2.00+0.00i	-2.00+0.00i	=S3	+ S3				
79	2	8.271548	2.00+0.00i	-2.00+0.00i	=S3	+ S3			79	2	8.276109	2.00+0.00i	2.00+0.00i	=S4	+ S4				
81	2	8.279647	2.00+0.00i	2.00+0.00i	=S4	+ S4			81	2	8.333843	2.00+0.00i	-2.00+0.00i	=S3	+ S3				
83	2	8.326988	2.00+0.00i	2.00+0.00i	=S4	+ S4			83	2	8.360803	2.00+0.00i	2.00+0.00i	=S4	+ S4				
...																			

FIG. 7: The calculated band representations of k -point P (a) and Q (b) as marked in Fig. 5(f). The number of total electrons is 80 in PdSb_2 .

R are shown in lower panels of Fig. 5. The R point is a k -point with nonsymmorphic symmetry in SG 205, where IRs of the space group can not be expressed as IRs of the corresponding point group multiplied by a phase factor. With the application of the program “irvsp”, the IRs at R are obtained. Figs. 6 (a-c) show the results of IRs for the low-energy bands. The number of total electrons is 80 for PdSb_2 . It is shown that the energy ordering of electron bands is changed at R under tiny strains.

The IRs at all the maximal HSK points can be computed directly by *irvsp* (which can also generate the trace file – “trace.txt”). By directly comparing these obtained IRs with the EBRs of the TQC theory (released on the BCS) and solving the compatibility relations, we can find that it is a topological insulating phase without strain, while it’s a symmetry-enforced semimetallic phase with tiny tensile strains.

To further obtain the crossing points in the system, we computed the IRs along the R–X line (named S [u,0.5,u] in the units of reciprocal lattice vectors). These points are also non-symmorphic, which are on the boundary of the 3D BZ for SG 205. The CRT for the S point is listed in Fig. S2. For the P and Q points in Fig. 5(f) of the strained crystal, we show the results of obtained IRs in Fig. 7. At the P point, the 79-80 degenerate bands are assigned to “S3+S3”, while 81-82 degenerate bands are assigned to “S4+S4”. However, at the Q point, the results are in the opposite way. Without doing further calculations with a denser kmesh between P and Q points, we can still conclude that it’s a real 4-fold crossing along R–X on the BZ boundary, which is robust against SOC. The double degeneracy is due to the presence of TRS. The symmetry #15 is the operator $g_y \equiv \{M_y | 0\frac{1}{2}\frac{1}{2}\}$. Therefore, the doubly-degenerate bands have the same g_y eigenvalue ($\{S3, S3\}$ or $\{S4, S4\}$), and the 4-fold crossing point along R–X is protected by g_y symmetry. As a result, the crossing 4-fold points actually form a Dirac nodal ring on the BZ boundary. Considering the full symmetry of SG 205, we conclude that there are three Dirac nodal rings in PdSb_2 with tiny strains, which can be further checked in experiments in the future.

B. Bismuth

As aforementioned, with the IRs at maximal HSK points obtained by “irvsp”, we can further check the topology by comparing them with the EBRs of the TQC theory. Here, we will take Bi as an example to briefly introduce the process. The element Bismuth has the rhombohedral structure of SG 166. The maximum HSK points of SG 166 are listed on the BCS, as Γ (GM), T, F, L. After performing the *ab-initio* calculations to obtain the eigen-wavefunctions at maximal HSK points, the obtained IRs of the occupied bands are given in Table III. From the TQC and BCS, the EBRs of SG 166 are obtained, as shown in Fig. 8. As there are only six valence bands, we can find that they are not belonging to any EBR induced from the $9d$ or $9e$ Wyckoff position. In the EBRs induced from the $3a$ and $3b$ Wyckoff

Wyckoff pos.	$3a(\bar{3}m)$	$3a(\bar{3}m)$	$3a(\bar{3}m)$	$3a(\bar{3}m)$	$3b(\bar{3}m)$	$3b(\bar{3}m)$	$3b(\bar{3}m)$	$3b(\bar{3}m)$	$9d(2/m)$	$9d(2/m)$	$9e(2/m)$	$9e(2/m)$
Band-Rep.	$^1E_g^2E_g \uparrow G(2)$	$^1E_u^2E_u \uparrow G(2)$	$\bar{E}_g \uparrow G(2)$	$\bar{E}_u \uparrow G(2)$	$^1E_g^2E_g \uparrow G(2)$	$^1E_u^2E_u \uparrow G(2)$	$\bar{E}_g \uparrow G(2)$	$\bar{E}_u \uparrow G(2)$	$^1E_g^2E_g \uparrow G(6)$	$^1E_u^2E_u \uparrow G(6)$	$^1E_g^2E_g \uparrow G(6)$	$^1E_u^2E_u \uparrow G(6)$
Decomposable/Indecomposable	Indecomposable	Indecomposable	Indecomposable	Indecomposable	Indecomposable	Indecomposable	Indecomposable	Indecomposable	Decomposable	Decomposable	Decomposable	Decomposable
$\Gamma:(0,0,0)$	$\Gamma_4F_5(2)$	$\bar{\Gamma}_6F_7(2)$	$\Gamma_8(2)$	$\bar{\Gamma}_9(2)$	$\Gamma_4F_5(2)$	$\bar{\Gamma}_6F_7(2)$	$\Gamma_8(2)$	$\bar{\Gamma}_9(2)$	$\Gamma_4F_5(2) \oplus 2\Gamma_8(2)$	$\bar{\Gamma}_6F_7(2) \oplus 2\bar{\Gamma}_9(2)$	$\Gamma_4F_5(2) \oplus 2\Gamma_8(2)$	$\bar{\Gamma}_6F_7(2) \oplus 2\bar{\Gamma}_9(2)$
$T:(0,0,3/2)$	$\bar{\Gamma}_4F_5(2)$	$\Gamma_6F_7(2)$	$\bar{\Gamma}_8(2)$	$\Gamma_9(2)$	$\bar{\Gamma}_4F_5(2)$	$\Gamma_6F_7(2)$	$\bar{\Gamma}_8(2)$	$\Gamma_9(2)$	$\bar{\Gamma}_4F_5(2) \oplus 2\bar{\Gamma}_9(2)$	$\Gamma_6F_7(2) \oplus 2\Gamma_8(2)$	$\bar{\Gamma}_4F_5(2) \oplus 2\bar{\Gamma}_9(2)$	$\Gamma_6F_7(2) \oplus 2\Gamma_8(2)$
$F:(0,1/2,1)$	$F_3F_4(2)$	$\bar{F}_3F_6(2)$	$F_3F_4(2)$	$\bar{F}_3F_6(2)$	$F_3F_4(2)$	$\bar{F}_3F_6(2)$	$F_3F_4(2)$	$\bar{F}_3F_6(2)$	$F_3F_4(2) \oplus 2F_3F_6(2)$	$2F_3F_4(2) \oplus F_3F_6(2)$	$F_3F_4(2) \oplus 2F_3F_6(2)$	$2F_3F_4(2) \oplus F_3F_6(2)$
$L:(-1/2,1/2,1/2)$	$L_3L_4(2)$	$\bar{L}_3L_6(2)$	$L_3L_4(2)$	$\bar{L}_3L_6(2)$	$L_3L_4(2)$	$\bar{L}_3L_6(2)$	$L_3L_4(2)$	$\bar{L}_3L_6(2)$	$2L_3L_4(2) \oplus L_3L_6(2)$	$L_3L_4(2) \oplus 2L_3L_6(2)$	$L_3L_4(2) \oplus 2L_3L_6(2)$	$2L_3L_4(2) \oplus L_3L_6(2)$

FIG. 8: A complete list of the EBRs of space group 166 in the presence of SOC. Each EBR is defined by a Maximal Wyckoff site (nx) and an IR of its site-symmetry group, which are indicated by the first and second rows, respectively. Then, the following rows present the IRs at the Maximal HSK points.

positions, we can find that the number of the pairs of F5F6 at F has to be the same as the total number of the IRs GM9 and GM6GM7 at Γ . In Bismuth, the obtained IRs have three IRs of F5F6, but neither GM9 nor GM6GM7. In conclusion, the set of occupied bands in Bismuth can not be expressed as any sum of EBRs in SG 166. In other words, it has to be topological [7].

TABLE III: The IRs at maximal HSK points obtained by *irvsp* in Bismuth. “(n)” indicates the degeneracy of the bands, while “[m]” indicates the total number of the computed bands at the k -point.

HSK	six valence bands
GM	GM8 (2); GM8 (2); GM4 GM5 (2); [6]
T	T9 (2); T8 (2); T6 T7 (2); [6]
F	F3 F4 (2); F5 F6 (2); F5 F6 (2); [6]
L	L3 L4 (2); L5 L6 (2); L5 L6 (2); [6]

VII. CONCLUSIONS

In summary, we presented an open-source software package called “*irvsp*” that determines the IRs of electronics states. It is very user-friendly and is written in Fortran 90/77, showing a powerful function to analyze the IRs for all the k -points in all 230 space groups. Thus, that also can classify BZ surface points for nonsymmorphic crystals. We showed how to use it to identify IRs and further get the topological property for a new material. As an example, we explored a new topological material PdSb₂, whose topology is very sensitive to the lattice parameter. Under tiny strains, it was identified as a four-fold Dirac nodal-line metal.

Acknowledgments We thank Dr. Peter Blaha and Dr. Luis Elcoro for sharing the character tables of 32 point groups implemented in the WIEN2k package and the character tables of 230 space groups for all k -points on the BCS. This work was supported by the National Natural Science Foundation of China (No. 11974395), the CAS Pioneer Hundred Talents Program, and the National Thousand-Young-Talents Program. Q. S. W. acknowledges the support of NCCR MARVEL.

-
- [1] B. A. Bernevig, T. L. Hughes, and S.-C. Zhang, *Science* **314**, 1757 (2006).
 - [2] M. König, S. Wiedmann, C. Brüne, A. Roth, H. Buhmann, L. W. Molenkamp, X.-L. Qi, and S.-C. Zhang, *Science* **318**, 766 (2007).
 - [3] C. L. Kane and E. J. Mele, *Physical review letters* **95**, 226801 (2005).
 - [4] B. A. Bernevig and S.-C. Zhang, *Physical review letters* **96**, 106802 (2006).
 - [5] C. Kane and M. Hasan, *Rev. Mod. Phys* **82**, 3045 (2010).
 - [6] X.-L. Qi and S.-C. Zhang, *Reviews of Modern Physics* **83**, 1057 (2011).
 - [7] F. Schindler, A. M. Cook, M. G. Vergniory, Z. Wang, S. S. Parkin, B. A. Bernevig, and T. Neupert, *Science advances* **4**, eaat0346 (2018).
 - [8] X. Wan, A. M. Turner, A. Vishwanath, and S. Y. Savrasov, *Physical Review B* **83**, 205101 (2011).
 - [9] B. J. Wieder, B. Bradlyn, Z. Wang, J. Cano, Y. Kim, H.-S. D. Kim, A. M. Rappe, C. Kane, and B. A. Bernevig, *Science* **361**, 246 (2018).
 - [10] F. Tang, H. C. Po, A. Vishwanath, and X. Wan, arXiv preprint arXiv:1807.09744 (2018).
 - [11] T. Zhang, Y. Jiang, Z. Song, H. Huang, Y. He, Z. Fang, H. Weng, and C. Fang, *Nature* **566**, 475 (2019).
 - [12] M. Vergniory, L. Elcoro, C. Felser, N. Regnault, B. A. Bernevig, and Z. Wang, *Nature* **566**, 480 (2019).
 - [13] Y. Xu, Z. Song, Z. Wang, H. Weng, and X. Dai, *Phys. Rev. Lett.* **122**, 256402 (2019), URL <https://link.aps.org/doi/10.1103/PhysRevLett.122.256402>.
 - [14] G. Li, B. Yan, Z. Wang, and K. Held, *Phys. Rev. B* **95**, 035102 (2017), URL <https://link.aps.org/doi/10.1103/PhysRevB.95.035102>.
 - [15] S. Nie, L. Xing, R. Jin, W. Xie, Z. Wang, and F. B. Prinz, *Phys. Rev. B* **98**, 125143 (2018), URL <https://link.aps.org/doi/10.1103/PhysRevB.98.125143>.
 - [16] Y. Qian, S. Nie, C. Yi, L. Kong, C. Fang, T. Qian, H. Ding, Y. Shi, Z. Wang, H. Weng, et al., *npj Computational Materials* **5**, 121 (2019), URL <https://doi.org/10.1038/s41524-019-0260-6>.
 - [17] H. Zhang, C.-X. Liu, X.-L. Qi, X. Dai, Z. Fang, and S.-C. Zhang, *Nature physics* **5**, 438 (2009).
 - [18] Y. Xia, D. Qian, D. Hsieh, L. Wray, A. Pal, H. Lin, A. Bansil, D. Grauer, Y. S. Hor, R. J. Cava, et al., *Nature physics* **5**, 398 (2009).

- [19] Y. Chen, J. G. Analytis, J.-H. Chu, Z. Liu, S.-K. Mo, X.-L. Qi, H. Zhang, D. Lu, X. Dai, Z. Fang, et al., *science* **325**, 178 (2009).
- [20] Z. Wang, Y. Sun, X.-Q. Chen, C. Franchini, G. Xu, H. Weng, X. Dai, and Z. Fang, *Physical Review B* **85**, 195320 (2012).
- [21] Z. Liu, B. Zhou, Y. Zhang, Z. Wang, H. Weng, D. Prabhakaran, S.-K. Mo, Z. Shen, Z. Fang, X. Dai, et al., *Science* **343**, 864 (2014).
- [22] Z. Wang, H. Weng, Q. Wu, X. Dai, and Z. Fang, *Phys. Rev. B* **88**, 125427 (2013), URL <https://link.aps.org/doi/10.1103/PhysRevB.88.125427>.
- [23] Z. Liu, J. Jiang, B. Zhou, Z. Wang, Y. Zhang, H. Weng, D. Prabhakaran, S. Mo, H. Peng, P. Dudin, et al., *Nature materials* **13**, 677 (2014).
- [24] H. Weng, C. Fang, Z. Fang, B. A. Bernevig, and X. Dai, *Physical Review X* **5**, 011029 (2015).
- [25] S.-M. Huang, S.-Y. Xu, I. Belopolski, C.-C. Lee, G. Chang, B. Wang, N. Alidoust, G. Bian, M. Neupane, C. Zhang, et al., *Nature communications* **6**, 7373 (2015).
- [26] B. Lv, H. Weng, B. Fu, X. Wang, H. Miao, J. Ma, P. Richard, X. Huang, L. Zhao, G. Chen, et al., *Physical Review X* **5**, 031013 (2015).
- [27] S.-Y. Xu, I. Belopolski, N. Alidoust, M. Neupane, G. Bian, C. Zhang, R. Sankar, G. Chang, Z. Yuan, C.-C. Lee, et al., *Science* **349**, 613 (2015).
- [28] T. H. Hsieh, H. Lin, J. Liu, W. Duan, A. Bansil, and L. Fu, *Nature communications* **3**, 982 (2012).
- [29] Y. Tanaka, Z. Ren, T. Sato, K. Nakayama, S. Souma, T. Takahashi, K. Segawa, and Y. Ando, *Nature Physics* **8**, 800 (2012).
- [30] Z. Wang, A. Alexandradinata, R. J. Cava, and B. A. Bernevig, *Nature* **532**, 189 (2016).
- [31] J. Ma, C. Yi, B. Lv, Z. Wang, S. Nie, L. Wang, L. Kong, Y. Huang, P. Richard, P. Zhang, et al., *Science advances* **3**, e1602415 (2017).
- [32] Z. Zhu, Y. Cheng, and U. Schwingenschlögl, *Physical Review B* **85**, 235401 (2012).
- [33] B. Bradlyn, L. Elcoro, J. Cano, M. Vergniory, Z. Wang, C. Felser, M. Aroyo, and B. A. Bernevig, *Nature* **547**, 298 (2017).
- [34] J. Cano, B. Bradlyn, Z. Wang, L. Elcoro, M. Vergniory, C. Felser, M. Aroyo, and B. A. Bernevig, *Physical Review B* **97**, 035139 (2018).
- [35] M. Vergniory, L. Elcoro, Z. Wang, J. Cano, C. Felser, M. Aroyo, B. A. Bernevig, and B. Bradlyn, *Physical Review E* **96**, 023310 (2017).
- [36] J. Cano, B. Bradlyn, Z. Wang, L. Elcoro, M. Vergniory, C. Felser, M. Aroyo, and B. A. Bernevig, *Physical review letters* **120**, 266401 (2018).
- [37] L. Elcoro, B. Bradlyn, Z. Wang, M. G. Vergniory, J. Cano, C. Felser, B. A. Bernevig, D. Orobengoa, G. Flor, and M. I. Aroyo, *Journal of Applied Crystallography* **50**, 1457 (2017).
- [38] M. I. Aroyo, J. Perez-Mato, D. Orobengoa, E. Tasci, G. De La Flor, and A. Kirov, *Bulg. Chem. Commun* **43**, 183 (2011).
- [39] H. T. Stokes, B. J. Campbell, and R. Cordes, *Acta Crystallographica Section A: Foundations of Crystallography* **69**, 388 (2013).
- [40] P. Blaha, K. Schwarz, G. K. Madsen, D. Kvasnicka, and J. Luitz, *An augmented plane wave+ local orbitals program for calculating crystal properties* (2001).
- [41] C. Persson, *Electronic structure of intrinsic and doped silicon carbide and silicon*, PhD thesis, ISBN 91-7219-442-1 (1999).
- [42] G. Kresse and J. Furthmüller, *Phys. Rev. B* **54**, 169 (1996).
- [43] N. Marzari, A. A. Mostofi, J. R. Yates, I. Souza, and D. Vanderbilt, *Rev. Mod. Phys.* **84**, 1419 (2012), URL <https://link.aps.org/doi/10.1103/RevModPhys.84.1419>.
- [44] A. A. Mostofi, J. R. Yates, G. Pizzi, Y.-S. Lee, I. Souza, D. Vanderbilt, and N. Marzari, *Computer Physics Communications* **185**, 2309 (2014).
- [45] Q. Wu, S. Zhang, H.-F. Song, M. Troyer, and A. A. Soluyanov, *Computer Physics Communications* **224**, 405 (2018), ISSN 0010-4655, URL <http://www.sciencedirect.com/science/article/pii/S0010465517303442>.
- [46] C. Yue, *Symmetrization of wannier tight-binding models*, https://github.com/quanshengwu/wannier_tools/tree/master/wannhr_symm.
- [47] D. Gresch, Q. Wu, G. W. Winkler, R. Häuselmann, M. Troyer, and A. A. Soluyanov, *Physical Review Materials* **2**, 103805 (2018).
- [48] J. C. Slater and G. F. Koster, *Phys. Rev.* **94**, 1498 (1954), URL <https://link.aps.org/doi/10.1103/PhysRev.94.1498>.
- [49] M. Willatzen and L. L. Y. Voon, *The kp Method-Electronic Properties of Semiconductors*, vol. 53 (SpringerBerlinHeidelberg,Berlin,Heidelberg, 2009).
- [50] J. F. Cornwell, *Group Theory in Physics [Vol. 1-2]*. (Academic Press, 1984).
- [51] H.-W. Streitwolf, *Group theory in solid-state physics* (Macdonald and Co., 1971).
- [52] B. Bradlyn, J. Cano, Z. Wang, M. Vergniory, C. Felser, R. J. Cava, and B. A. Bernevig, *Science* **353**, aaf5037 (2016).
- [53] R. Chapai, Y. Jia, W. Shelton, R. Nepal, M. Saghayezhian, J. DiTusa, E. Plummer, C. Jin, and R. Jin, *Physical Review B* **99**, 161110 (2019).
- [54] J. Pratt, K. Myles, J. Darby Jr, and M. Mueller, *Journal of the Less Common Metals* **14**, 427 (1968).
- [55] S. Furuseth, K. Selte, A. Kjekshus, P. Nielsen, B. Sjöberg, and E. Larsen, *Acta Chem. Scand* **19** (1965).
- [56] N. E. Brese and H. G. von Schnering, *Zeitschrift für anorganische und allgemeine Chemie* **620**, 393 (1994).

APPENDIX

1. `tbbox.in` for Bi_2Se_3

```

case = soc ! lda or soc

proj:
orbt = 2
ntau = 5
0.39900000 0.39900000 0.39900000 1 3 ! x1, x2, x3, itau, iorbit
0.60100000 0.60100000 0.60100000 1 3
0.20600000 0.20600000 0.20600000 2 3
0.79400000 0.79400000 0.79400000 2 3
0.00000000 0.00000000 0.00000000 2 3
end projections

kpoint:
kmesh = 10
Nk = 3
0.00000000 0.00000000 0.00000000 ! k0: y1,y2,y3
0.50000000 0.50000000 0.50000000 ! k1
0.50000000 0.50000000 0.00000000 ! k2
0.00000000 0.50000000 0.00000000 ! k3
end kpoint_path

unit_cell:
1.194537707 -2.069000000 9.546666657 0.139523990 -0.241662639 0.034916201 ! b1x b1y b1z; g1x g1y g1z
1.194537707 2.069000000 9.546666657 0.139523990 0.241662639 0.034916201
-2.389075414 0.000000000 9.546666657 -0.279047979 0.000000000 0.034916201
1 1.000000 0.000000 1.000000 0.000000 0.000000 0.000000 0.000000 0.000000 ! SN,Det,omega,nx,ny,nz,v1,v2,v3
2 -1.000000 0.000000 1.000000 0.000000 0.000000 0.000000 0.000000 0.000000
3 1.000000 180.000000 0.866025 0.500000 0.000000 0.000000 0.000000 0.000000
4 -1.000000 180.000000 0.866025 0.500000 0.000000 0.000000 0.000000 0.000000
5 1.000000 120.000000 0.000000 0.000000 -1.000000 0.000000 0.000000 0.000000
6 -1.000000 120.000000 0.000000 0.000000 -1.000000 0.000000 0.000000 0.000000
7 1.000000 179.999999 0.000000 1.000000 0.000000 0.000000 0.000000 0.000000
8 -1.000000 179.999999 0.000000 1.000000 0.000000 0.000000 0.000000 0.000000
9 1.000000 120.000000 0.000000 0.000000 1.000000 0.000000 0.000000 0.000000
10 -1.000000 120.000000 0.000000 0.000000 1.000000 0.000000 0.000000 0.000000
11 1.000000 180.000000 0.866025 -0.500000 0.000000 0.000000 0.000000 0.000000
12 -1.000000 180.000000 0.866025 -0.500000 0.000000 0.000000 0.000000 0.000000
end unit_cell

```

TABLE S1: A list of codes are available in the repository: <https://github.com/zjwang11/irvsp/>. Different versions of the codes can be developed based on the different types of the WFs and conventions of the CRTs. Besides the `src_irvsp_v2.tar.gz` code mainly discussed in the main text, there are more codes developed.

	CRTs	PNG	BCS
WFs			
PW basis		src_irvsp_v1.tar.gz	src_irvsp_v2.tar.gz
TB basis		src_ir2tb_v1.tar.gz	src_ir2tb_v2.tar.gz

2. The brief description of inputs for “ir2tb”

Based on the different types of the WFs and conventions of the CRTs, different versions of the codes are developed, as shown in Table S1. The program “ir2tb” is based on the TB WFs. BLAS and LAPACK linear algebra libraries are needed to diagonalize the TB Hamiltonian. It needs two input files: *tbbbox.in* and *case_hr.dat*.

The *case_hr.dat* file, containing the TB parameters in Wannier90 format [43], may be generated by the software Wannier90 [44] with symmetrization [47], or generated by users with a toy TB model, or generated from Slater-Koster method [48] or a discretization of $k \cdot p$ model onto a lattice [49].

The *tbbbox.in* file provides detailed information about the TB Hamiltonian (*i.e.*, the *case_hr.dat* file), which is an essential input for the program “ir2tb”. The tag *case = lda* (*case = soc*) indicates that the TB Hamiltonian does not (does) have the SOC effect. The *lda/soc_hr.dat* is needed accordingly. In the “proj” block, “orbt=1 or 2” indicates the convention of the local basis ordering on each atom. The local orbitals in convention 1 are listed in Table S3, while those in convention 2 are in the order as implemented in Wannier90. “ntau” indicates the total number of the atoms in the TB Hamiltonian, which also means how many lines follow in this block. The local orbitals of the TB Hamiltonian are provided by : ‘x1,x2,x3, itau, iorbit’. ‘x1,x2,x3’ stand for the positions of atoms: $\tau_i = (x_1\mathbf{t}_1, x_2\mathbf{t}_2, x_3\mathbf{t}_3)$; “itau” stand for the kinds of atoms; and “iorbit” stand for the total number of local orbitals on each atom. So far, “irobit” is limited to the values of [1,3,5,4,6,7,8,9], whose detailed orbital informations are provided in Table S3. In the case of *case = soc*, the local orbitals will be doubled automatically: the first half are spin-up and the second half are spin-down. In the “kpoint” block, the k -path is given as $k_0 - k_1 - \dots - k_N$ with *kmesh* on each segment. The “unit.cell” block gives the lattice vectors and reciprocal lattice vectors in first three lines, followed by space group operators of the system we considered. They are the same lines as the program “irvsp” reads in OUTCAR file.

TABLE S2: A brief summary of *tbbbox.in*.

Comments	Descriptions
! lda or soc	lda: nspin=1 (without SOC); soc: nspin=2 (with SOC)
! x1,x2,x3,itau,iorbit	defining $\tau_i = (x_1\mathbf{t}_1, x_2\mathbf{t}_2, x_3\mathbf{t}_3)$, iorbit $\in \{1, 3, 4, 5, 6, 7, 8, 9\}$
! k0: y1,y2,y3	defining $\mathbf{k}_0 = (y_1\mathbf{g}_1, y_2\mathbf{g}_2, y_3\mathbf{g}_3)$; kpath is along $\mathbf{k}_0 - \mathbf{k}_1 - \dots - \mathbf{k}_n$.
! b1x b1y b1z; g1x g1y g1z	defining $\mathbf{t}_1 = (b_{1x}\hat{x}, b_{1y}\hat{y}, b_{1z}\hat{z})$; $\mathbf{g}_1 = 2\pi(g_{1x}\hat{x}, g_{1y}\hat{y}, g_{1z}\hat{z})$
! SN,Det,omega,nx,ny,nz,v1,v2,v3	defining $\mathcal{O} = \{R \mathbf{v}\}$ with $R = \text{Det} \cdot e^{-i\omega(\vec{n} \cdot \vec{L})}$ and $\mathbf{v} = (v_1\mathbf{t}_1, v_2\mathbf{t}_2, v_3\mathbf{t}_3)$. SN stands for the sequential number.

TABLE S3: The local orbitals in convention 1 (orbt=1) are given in the table.

iorbit	local orbitals	D rep. in Eq. (7)
1	s	$D^1 = 1$
3	p_x, p_y, p_z	$D^3 = \text{Det} \cdot e^{-i\omega(\vec{n} \cdot \vec{L})}$
5	$d_{xy}, d_{yz}, d_{zx}, d_{x^2-y^2}, d_{3z^2-r^2}$	$D^5 = e^{-i\omega(\vec{n} \cdot \vec{F})}$
4	s, p_x, p_y, p_z	$D^4 = D^1 \oplus D^3$
6	$s, d_{xy}, d_{yz}, d_{zx}, d_{x^2-y^2}, d_{3z^2-r^2}$	$D^6 = D^1 \oplus D^5$
8	$p_x, p_y, p_z, d_{xy}, d_{yz}, d_{zx}, d_{x^2-y^2}, d_{3z^2-r^2}$	$D^8 = D^3 \oplus D^5$
9	$s, p_x, p_y, p_z, d_{xy}, d_{yz}, d_{zx}, d_{x^2-y^2}, d_{3z^2-r^2}$	$D^9 = D^1 \oplus D^3 \oplus D^5$
7	$f_{xyz}, f_{5x^3-xr^2}, f_{5y^3-yr^2}, f_{5z^3-zr^2}, f_{x(y^2-z^2)}, f_{y(z^2-r^2)}, f_{z(x^2-y^2)}$	$D^7 = \text{Det} \cdot e^{-i\omega(\vec{n} \cdot \vec{F})}$

$$P_x = \begin{pmatrix} 0 & 0 & -i & 0 & 0 \\ 0 & 0 & 0 & -i & -i\sqrt{3} \\ i & 0 & 0 & 0 & 0 \\ 0 & i & 0 & 0 & 0 \\ 0 & i\sqrt{3} & 0 & 0 & 0 \end{pmatrix}; P_y = \begin{pmatrix} 0 & i & 0 & 0 & 0 \\ -i & 0 & 0 & 0 & 0 \\ 0 & 0 & 0 & -i & i\sqrt{3} \\ 0 & 0 & i & 0 & 0 \\ 0 & 0 & -i\sqrt{3} & 0 & 0 \end{pmatrix}; P_z = \begin{pmatrix} 0 & 0 & 0 & 2i & 0 \\ 0 & 0 & i & 0 & 0 \\ 0 & -i & 0 & 0 & 0 \\ -2i & 0 & 0 & 0 & 0 \\ 0 & 0 & 0 & 0 & 0 \end{pmatrix}$$

$$F_x = \begin{pmatrix} 0 & 0 & 0 & 0 & 2i & 0 & 0 \\ 0 & 0 & 0 & 0 & 0 & 0 & 0 \\ 0 & 0 & 0 & \frac{3i}{2} & 0 & 0 & \frac{i\sqrt{15}}{2} \\ 0 & 0 & -\frac{3i}{2} & 0 & 0 & \frac{i\sqrt{15}}{2} & 0 \\ -2i & 0 & 0 & 0 & 0 & 0 & 0 \\ 0 & 0 & 0 & -\frac{i\sqrt{15}}{2} & 0 & 0 & -\frac{i}{2} \\ 0 & 0 & -\frac{i\sqrt{15}}{2} & 0 & 0 & \frac{i}{2} & 0 \end{pmatrix} \quad (19)$$

$$F_y = \begin{pmatrix} 0 & 0 & 0 & 0 & 0 & 2i & 0 \\ 0 & 0 & 0 & -\frac{3i}{2} & 0 & 0 & \frac{i\sqrt{15}}{2} \\ 0 & 0 & 0 & 0 & 0 & 0 & 0 \\ 0 & \frac{3i}{2} & 0 & 0 & \frac{i\sqrt{15}}{2} & 0 & 0 \\ 0 & 0 & 0 & -\frac{i\sqrt{15}}{2} & 0 & 0 & \frac{i}{2} \\ -2i & 0 & 0 & 0 & 0 & 0 & 0 \\ 0 & -\frac{i\sqrt{15}}{2} & 0 & 0 & -\frac{i}{2} & 0 & 0 \end{pmatrix} \quad (20)$$

$$F_z = \begin{pmatrix} 0 & 0 & 0 & 0 & 0 & 0 & 2i \\ 0 & 0 & \frac{3i}{2} & 0 & 0 & \frac{i\sqrt{15}}{2} & 0 \\ 0 & -\frac{3i}{2} & 0 & 0 & \frac{i\sqrt{15}}{2} & 0 & 0 \\ 0 & 0 & 0 & 0 & 0 & 0 & 0 \\ 0 & 0 & -\frac{i\sqrt{15}}{2} & 0 & 0 & -\frac{i}{2} & 0 \\ 0 & -\frac{i\sqrt{15}}{2} & 0 & 0 & \frac{i}{2} & 0 & 0 \\ -2i & 0 & 0 & 0 & 0 & 0 & 0 \end{pmatrix} \quad (21)$$

3. The transformation from the standard conventional unit to the primitive unit cell

The maximal HSK points from the BCS are given in the convention reciprocal lattice vectors, while the lattice vectors in VASP usually are given in the primitive cell. The transformation depends on the type of the lattice. There are only seven different types of lattices, *i.e.* P, C, B, A, R, F and I . In the X type, the primitive lattices $(\vec{p}_1, \vec{p}_2, \vec{p}_3)$ are defined by a transformation matrix M_X .

$$(\vec{p}_1 \ \vec{p}_2 \ \vec{p}_3) = (\vec{c}_1 \ \vec{c}_2 \ \vec{c}_3) \cdot M_X \quad (22)$$

where \vec{c}_1, \vec{c}_2 and \vec{c}_3 are the standard conventional lattices. In the program, all the matrices M_X are given as follows:

$$M_P = \begin{pmatrix} 1 & 0 & 0 \\ 0 & 1 & 0 \\ 0 & 0 & 1 \end{pmatrix}; M_C = \begin{pmatrix} 0.5 & 0.5 & 0 \\ -0.5 & 0.5 & 0 \\ 0 & 0 & 1 \end{pmatrix}; M_B = \begin{pmatrix} 0.5 & 0 & -0.5 \\ 0 & 1 & 0 \\ 0.5 & 0 & 0.5 \end{pmatrix}; M_A = \begin{pmatrix} 1 & 0 & 0 \\ 0 & 0.5 & -0.5 \\ 0 & 0.5 & 0.5 \end{pmatrix};$$

$$M_R = \begin{pmatrix} 2/3 & -1/3 & -1/3 \\ 1/3 & 1/3 & -2/3 \\ 1/3 & 1/3 & 1/3 \end{pmatrix}; M_F = \begin{pmatrix} 0 & 0.5 & 0.5 \\ 0.5 & 0 & 0.5 \\ 0.5 & 0.5 & 0 \end{pmatrix}; M_I = \begin{pmatrix} -0.5 & 0.5 & 0.5 \\ 0.5 & -0.5 & 0.5 \\ 0.5 & 0.5 & -0.5 \end{pmatrix}.$$

4. The character tables for R -little group and S -little group

Figs. S1 and S2 show the character tables for R -little group and S -little group, respectively. At the k -point $[(u, v, w)$ given in the conventional reciprocal basis], the block $\begin{matrix} x + iy \\ a & b & c \end{matrix}$ corresponds to a complex value of $(x + iy) \cdot \exp[i\pi(au + bv + cw)]$.

The k-point name is R
 24 symmetry operations (module lattice translations) in the R-little group of space sgroup 205
 We do NOT classify the elements into classes.
 Table can be found on website: <http://www.cryst.ehu.es/>.

2 R : kname 0.50 0.50 0.50 : given in the conventional basis
 1 : the exsistance of antiunitary symmetry. 1-exist; 0-no

Reality		1	2	3	4	5	6	7	8	9	10	11	12
0	R1+	2.00+0.00i	0.00+0.00i	0.00+0.00i	0.00+0.00i	0.50+0.87i	0.50+0.87i	0.50+0.87i	0.50+0.87i	0.50-0.87i	-0.50+0.87i	-0.50+0.87i	-0.50+0.87i
0	R1-	2.00+0.00i	0.00+0.00i	0.00+0.00i	0.00+0.00i	0.50+0.87i	0.50+0.87i	0.50+0.87i	0.50+0.87i	0.50-0.87i	-0.50+0.87i	-0.50+0.87i	-0.50+0.87i
-1	R2+	2.00+0.00i	0.00+0.00i	0.00+0.00i	0.00+0.00i	-1.00+0.00i	-1.00+0.00i	-1.00+0.00i	-1.00+0.00i	-1.00+0.00i	1.00+0.00i	1.00+0.00i	1.00+0.00i
-1	R2-	2.00+0.00i	0.00+0.00i	0.00+0.00i	0.00+0.00i	-1.00+0.00i	-1.00+0.00i	-1.00+0.00i	-1.00+0.00i	-1.00+0.00i	1.00+0.00i	1.00+0.00i	1.00+0.00i
0	R3+	2.00+0.00i	0.00+0.00i	0.00+0.00i	0.00+0.00i	0.50-0.87i	0.50-0.87i	0.50-0.87i	0.50-0.87i	0.50+0.87i	-0.50-0.87i	-0.50-0.87i	-0.50-0.87i
0	R3-	2.00+0.00i	0.00+0.00i	0.00+0.00i	0.00+0.00i	0.50-0.87i	0.50-0.87i	0.50-0.87i	0.50-0.87i	0.50+0.87i	-0.50-0.87i	-0.50-0.87i	-0.50-0.87i

1	R4	1.00+0.00i	-1.00+0.00i	-1.00+0.00i	-1.00+0.00i	-1.00+0.00i	-1.00+0.00i	-1.00+0.00i	-1.00+0.00i	-1.00+0.00i	1.00+0.00i	1.00+0.00i	1.00+0.00i
0	R5	1.00+0.00i	-1.00+0.00i	-1.00+0.00i	-1.00+0.00i	0.50-0.87i	0.50-0.87i	0.50-0.87i	0.50-0.87i	0.50+0.87i	-0.50-0.87i	-0.50-0.87i	-0.50-0.87i
0	R6	1.00+0.00i	-1.00+0.00i	-1.00+0.00i	-1.00+0.00i	0.50+0.87i	0.50+0.87i	0.50+0.87i	0.50+0.87i	0.50-0.87i	-0.50+0.87i	-0.50+0.87i	-0.50+0.87i
1	R7	1.00+0.00i	-1.00+0.00i	-1.00+0.00i	-1.00+0.00i	-1.00+0.00i	-1.00+0.00i	-1.00+0.00i	-1.00+0.00i	-1.00+0.00i	1.00+0.00i	1.00+0.00i	1.00+0.00i
0	R8	1.00+0.00i	-1.00+0.00i	-1.00+0.00i	-1.00+0.00i	0.50-0.87i	0.50-0.87i	0.50-0.87i	0.50-0.87i	0.50+0.87i	-0.50-0.87i	-0.50-0.87i	-0.50-0.87i
0	R9	1.00+0.00i	-1.00+0.00i	-1.00+0.00i	-1.00+0.00i	0.50+0.87i	0.50+0.87i	0.50+0.87i	0.50+0.87i	0.50-0.87i	-0.50+0.87i	-0.50+0.87i	-0.50+0.87i
1	R10	3.00+0.00i	1.00+0.00i	1.00+0.00i	1.00+0.00i	0.00+0.00i	0.00+0.00i	0.00+0.00i	0.00+0.00i	0.00+0.00i	0.00+0.00i	0.00+0.00i	0.00+0.00i
1	R11	3.00+0.00i	1.00+0.00i	1.00+0.00i	1.00+0.00i	0.00+0.00i	0.00+0.00i	0.00+0.00i	0.00+0.00i	0.00+0.00i	0.00+0.00i	0.00+0.00i	0.00+0.00i

		13	14	15	16	17	18	19	20	21	22	23	24
		2.00+0.00i	0.00+0.00i	0.00+0.00i	0.00+0.00i	0.50+0.87i	0.50+0.87i	0.50+0.87i	0.50+0.87i	0.50-0.87i	-0.50+0.87i	-0.50+0.87i	-0.50+0.87i
		-2.00+0.00i	0.00+0.00i	0.00+0.00i	0.00+0.00i	-0.50-0.87i	-0.50-0.87i	-0.50-0.87i	-0.50-0.87i	-0.50+0.87i	0.50-0.87i	0.50-0.87i	0.50-0.87i
		2.00+0.00i	0.00+0.00i	0.00+0.00i	0.00+0.00i	-1.00+0.00i	-1.00+0.00i	-1.00+0.00i	-1.00+0.00i	-1.00+0.00i	1.00+0.00i	1.00+0.00i	1.00+0.00i
		-2.00+0.00i	0.00+0.00i	0.00+0.00i	0.00+0.00i	1.00+0.00i	1.00+0.00i	1.00+0.00i	1.00+0.00i	1.00+0.00i	-1.00+0.00i	-1.00+0.00i	-1.00+0.00i
		2.00+0.00i	0.00+0.00i	0.00+0.00i	0.00+0.00i	0.50-0.87i	0.50-0.87i	0.50-0.87i	0.50-0.87i	0.50+0.87i	-0.50-0.87i	-0.50-0.87i	-0.50-0.87i
		-2.00+0.00i	0.00+0.00i	0.00+0.00i	0.00+0.00i	-0.50+0.87i	-0.50+0.87i	-0.50+0.87i	-0.50+0.87i	-0.50-0.87i	0.50+0.87i	0.50+0.87i	0.50+0.87i

		1.00+0.00i	-1.00+0.00i	-1.00+0.00i	-1.00+0.00i	-1.00+0.00i	-1.00+0.00i	-1.00+0.00i	-1.00+0.00i	-1.00+0.00i	1.00+0.00i	1.00+0.00i	1.00+0.00i
		1.00+0.00i	-1.00+0.00i	-1.00+0.00i	-1.00+0.00i	0.50-0.87i	0.50-0.87i	0.50-0.87i	0.50-0.87i	0.50+0.87i	-0.50-0.87i	-0.50-0.87i	-0.50-0.87i
		1.00+0.00i	-1.00+0.00i	-1.00+0.00i	-1.00+0.00i	0.50+0.87i	0.50+0.87i	0.50+0.87i	0.50+0.87i	0.50-0.87i	-0.50+0.87i	-0.50+0.87i	-0.50+0.87i
		-1.00+0.00i	1.00+0.00i	1.00+0.00i	1.00+0.00i	1.00+0.00i	1.00+0.00i	1.00+0.00i	1.00+0.00i	1.00+0.00i	-1.00+0.00i	-1.00+0.00i	-1.00+0.00i
		-1.00+0.00i	1.00+0.00i	1.00+0.00i	1.00+0.00i	-0.50+0.87i	-0.50+0.87i	-0.50+0.87i	-0.50+0.87i	-0.50-0.87i	0.50-0.87i	0.50+0.87i	0.50+0.87i
		-1.00+0.00i	1.00+0.00i	1.00+0.00i	1.00+0.00i	-0.50-0.87i	-0.50-0.87i	-0.50-0.87i	-0.50-0.87i	-0.50+0.87i	0.50-0.87i	0.50-0.87i	0.50-0.87i
		3.00+0.00i	1.00+0.00i	1.00+0.00i	1.00+0.00i	0.00+0.00i	0.00+0.00i	0.00+0.00i	0.00+0.00i	0.00+0.00i	0.00+0.00i	0.00+0.00i	0.00+0.00i
		-3.00+0.00i	-1.00+0.00i	-1.00+0.00i	-1.00+0.00i	0.00+0.00i	0.00+0.00i	0.00+0.00i	0.00+0.00i	0.00+0.00i	0.00+0.00i	0.00+0.00i	0.00+0.00i

FIG. S1: The CRT of R -little group in the BCS convention.

The k-point name is S
 2 symmetry operations (module lattice translations) in the S-little group of space sgroup 205
 We do NOT classify the elements into classes.
 Table can be found on website: <http://www.cryst.ehu.es/>.

12 S : kname u 0.50 u : given in the conventional basis
 1 : the exsistance of antiunitary symmetry. 1-exist; 0-no

Reality		1	15
0	S1	1.00+0.00i	1.00+0.00i 1.0 0.0 0.0
0	S2	1.00+0.00i	-1.00+0.00i 1.0 0.0 0.0

1	S3	1.00+0.00i	0.00-1.00i 1.0 0.0 0.0
1	S4	1.00+0.00i	0.00+1.00i 1.0 0.0 0.0

FIG. S2: The CRT of S -little group in the BCS convention.